Environmental Science & Technology

pubs.acs.org/est

Article

Quantifying Methane and Ozone Precursor Emissions from Oil and Gas Production Regions across the Contiguous US

Colby B. Francoeur, Brian C. McDonald,* Jessica B. Gilman, Kyle J. Zarzana, Barbara Dix, Steven S. Brown, Joost A. de Gouw, Gregory J. Frost, Meng Li, Stuart A. McKeen, Jeff Peischl, Ilana B. Pollack, Thomas B. Ryerson, Chelsea Thompson, Carsten Warneke, and Michael Trainer

Cite This: *Environ. Sci. Technol.* 2021, 55, 9129−9139

Read Online

ACCESS | Metrics & More | Article Recommendations | Supporting Information

ABSTRACT: We present an updated fuel-based oil and gas (FOG) inventory with estimates of nitrogen oxide (NO_x) emissions from oil and natural gas production in the contiguous US (CONUS). We compare the FOG inventory with aircraft-derived ("top-down") emissions for NO_x over footprints that account for ∼25% of US oil and natural gas production. Across CONUS, we find that the bottom-up FOG inventory combined with other anthropogenic emissions is on average within ∼10% of top-down aircraft-derived NO_x emissions. We also find good agreement in the trends of NO_x from drilling- and production-phase activities, as inferred by satellites and in the bottom-up inventory. Leveraging tracer−tracer relationships derived from aircraft observations, methane (CH_4) and non-methane volatile organic compound (NMVOC) emissions have been added to the inventory. Our total CONUS emission estimates for 2015 of oil and natural gas are 0.45 ± 0.14 Tg NO_x/yr, 15.2 ± 3.0 Tg CH_4/yr, and 5.7 ± 1.7 Tg NMVOC/yr. Compared to the US National Emissions Inventory and Greenhouse Gas Inventory, FOG NO_x emissions are ∼40% lower, while inferred CH_4 and NMVOC emissions are up to a factor of ∼2 higher. This suggests that NMVOC/NO_x emissions from oil and gas basins are ∼3 times higher than current estimates and will likely affect how air quality models represent ozone formation downwind of oil and gas fields.

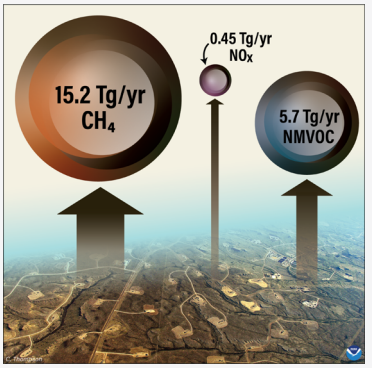

KEYWORDS: *oil and gas, emissions, energy production, methane, non-methane volatile organic compounds, nitrogen oxides, climate, air quality*

INTRODUCTION

In the past decade, production of oil and natural gas in the Unites States has increased by 50 and 100%, respectively (Figure S1),[1] and the production of both oil and natural gas is projected to continue increasing over the next decade. As production rises, so does the importance of quantifying emissions released during drilling and production. Carbon dioxide (CO_2) and methane (CH_4) are two greenhouse gases released during oil and natural gas production. Nitrogen oxides (NO_x = NO + NO_2) are co-emitted with CO_2 during combustion. The release of CH_4 and non-methane volatile organic compounds (NMVOCs) mostly arises due to fugitive leaks, making them difficult to quantify. CH_4 is the second largest anthropogenic greenhouse gas forcing on climate behind CO_2.[2] Around 85% of the CH_4 emissions released to the atmosphere due to oil and gas production are estimated to occur during production, gathering, and processing rather than in transmission, storage, and distribution systems,[3] although leaks in urban areas may be significantly underestimated.[4] Here, we focus on emissions occurring during the production, gathering, and processing phases of oil and natural gas production. Alvarez et al.[3] report that CH_4 emissions during oil and gas production are 60% higher than the Environmental Protection Agency's (EPA) Greenhouse Gas Inventory (GHGI). Significant uncertainties in these emissions remain both in absolute magnitude and in trends.[3,5−8] Properly quantifying the emissions is an important step toward understanding the impacts of energy production on climate.

Oil and gas production also impacts air quality through NO_x and NMVOC emissions that act as precursors to ozone (O_3) formation. Ozone in the troposphere has adverse effects on human health and air quality.[9,10] Oil and gas production activities have been shown to contribute to ozone formation in the Colorado Front Range,[11] as well as contribute to high wintertime ozone in the Uinta Basin, UT.[12−14] The underestimation of CH_4 emissions from fugitive leaks strongly suggests that NMVOC emissions are also underestimated.[15−18] Furthermore, cities such as Denver that are adjacent to oil and

Received: October 30, 2020
Revised: June 10, 2021
Accepted: June 11, 2021
Published: June 23, 2021

https://doi.org/10.1021/acs.est.0c07352
Environ. Sci. Technol. 2021, 55, 9129−9139

gas production fields may be impacted by NMVOC emissions when reacted with urban NO_x emissions.[16,19,20] High NMVOC concentrations in multiple regions have been linked to oil and gas activities.[21−24] Emissions of NO_x are from flaring and an array of engines used to extract and produce oil and gas. When compared to atmospherically derived flux estimates, Gorchov Negron et al.[25] showed that the US National Emissions Inventory (NEI) tends to overestimate NO_x emissions from the oil and gas sector, although the overestimates are not uniform. Trends of ozone precursor emissions from the oil and gas sector are also not well understood, as there is a lack of ground-based routine monitoring in oil- and gas-producing regions.[26] Satellite-based studies have shown increasing NO_x over a few isolated oil- and gas-producing regions.[27−29] Augmenting ground-based monitoring with satellite-based monitoring provides a more comprehensive system for tracking trends in oil and natural gas emissions. The capability of satellites has improved over time in terms of spatial resolution, such as from the ozone monitoring instrument (OMI: 13 km × 24 km, launched 2004)[30] to the tropospheric ozone monitoring instrument (TROPOMI: 3.5 km × 7 km retrievals, launched 2017).[31] Additionally, TROPOMI has detected enhancements in CH_4 from oil- and gas-producing regions, along with NO_2 and formaldehyde.[32] The visible infrared imaging radiometer suite (VIIRS) has been utilized to quantify the amount of natural gas flaring.[33]

In this study, we seek to improve the quantification of oil and natural gas emissions at a national scale by leveraging aircraft data from field campaigns investigating oil and gas regions, including the Uinta Basin Wintertime Ozone Study (UBWOS) in 2012, the Southeast Nexus Study (SENEX) in 2013, and the Shale Oil and Natural Gas Nexus Study (SONGNEX) in 2015. UBWOS focused on the Uinta Basin in Utah, SENEX covered the Marcellus as well as basins located in the Southeastern US, and SONGNEX covered most basins from Texas up to North Dakota. The regions covered during these campaigns are shown in Figures S2−S11. While we estimate oil and gas emissions in multiple years, we focus on 2015 due to SONGNEX having the most comprehensive data over oil- and gas-producing regions. The combined flights measured a footprint that accounts for ∼25% of US oil and natural gas production in 2015. Most prior studies quantifying NO_x and NMVOC emissions from oil and natural gas have mainly focused on individual regions or basins.[11,12,16,17] Here, we expand the previously developed fuel-based oil and gas (FOG) inventory over the contiguous US (CONUS). We leverage tracer−tracer ratios to estimate co-emitted CH_4 and NMVOCs along with NO_x and assess current regulatory inventories. The main significance of this study lies in providing a robust observational constraint on VOC/NO_x emissions from US oil and gas operations, a critical parameter in the formation of ground-level O_3. We also made publicly available our 2015 gridded emission maps, which can be utilized in future chemical transport modeling studies to assess air quality impacts.

METHODS

Fuel-Based Inventory of Oil and Gas NO_x. The FOG inventory was previously developed as an inventory of NO_x emissions from drilling, production, and processing of oil and natural gas.[25] Engine activity is estimated utilizing publicly available fuel sales data for off-road diesel fuel use[34] by oil and gas companies in the drilling phase and natural gas[35] (or lease fuel) consumed in the production phase by wellhead compressors, lateral compressors, dehydrators, heaters, and artificial lifts. These sales data are available at a state level. We then allocate fuel use spatially at a 4 × 4 km resolution by using facility-level data from Enverus DrillingInfo.[1] Drilling locations are determined by using well locations and spud (start of drilling) dates, while we allocate lease fuel using well production information.

For the production phase, the methodology is similar, but there are multiple types of engines and heaters employed in production.[36] Artificial lifts increase oil production in each well. Heaters are used during both oil and gas production for a variety of reasons. Mainly, they are used to prepare a stream for separation, keep pipes safe from hydrate formation, and storage. Lateral compressors gather and compress natural gas, while wellhead compressors are used to increase production at a natural gas well. Dehydrators are used to remove hydrates that cause pipeline corrosion. We allocate lease fuel to artificial lifts, dehydrators, and heaters based on whether a well produces oil and/or natural gas. Artificial lifts are only used when a well is producing oil, while dehydrators are only used if a well is producing natural gas. Heaters are used in both oil and natural gas production to varying extents, and the difference is accounted for in the inventory. We allocate the fuel consumed by compressors using county-level information from EPA's 2014 Oil and Gas Tool,[37] which reports the fraction of wellhead and lateral compressors required. We also account for NO_x emission controls (e.g., catalysts) on compressor engines using the oil and gas tool, which reports the fraction of compressors with NO_x emission controls at a county level.[37] Lastly, we convert the apportioned fuel to NO_x using eqs S1−S6 in the Supporting Information. A summary of fuel use and NO_x emission factors utilized in this study for individual basins is provided in Figures S2−S11.

Previously, FOG was mapped for only four basins in the US (Uinta, UT; Haynesville, TX; Marcellus, PA; and Fayetteville, AR). Here, we expand FOG to the CONUS between the years of 2012 and 2018, which coincide with the NOAA P3 SENEX 2013 and SONGNEX 2015 studies. We also add natural gas flaring emissions to FOG utilizing the volume of flared gas determined by the VIIRS instrument[33] multiplied with NO_x emission factors of flaring using eq S7 in the Supporting Information.[38] A limitation of our study is the use of a NO_x emission factor from an industrial flare, which likely underestimates the amount of NO_x thermally generated from an oil and gas flare by possibly a factor of ∼2, which burns at higher temperatures.[39] Figure 1 shows a map of the 2015 FOG NO_x emissions with boxes denoting where aircraft-derived "top-down" estimates of emissions have been calculated utilizing mass balance methods described below.[40−42] We use observational data from UBWOS 2012, SENEX 2013, and SONGNEX 2015 field campaigns to evaluate the FOG inventory.

Deriving FOG Emissions of CH_4 and NMVOCs. The basis for estimating CH_4 and NMVOC emissions from fugitive leaks is derived from tracer/tracer ratios measured by the NOAA P3 aircraft during the SENEX 2013 and SONGNEX 2015 field campaigns. Gorchov Negron et al.[25] previously showed a consistent correlation between CH_4 and NO_x emissions across oil- and gas-producing regions. While NO_x is emitted due to combustion and CH_4 is through fugitive leaks in equipment, the co-location of oil and gas NO_x and CH_4 emissions tends to lead to statistically significant correlations

https://doi.org/10.1021/acs.est.0c07352
Environ. Sci. Technol. 2021, 55, 9129−9139

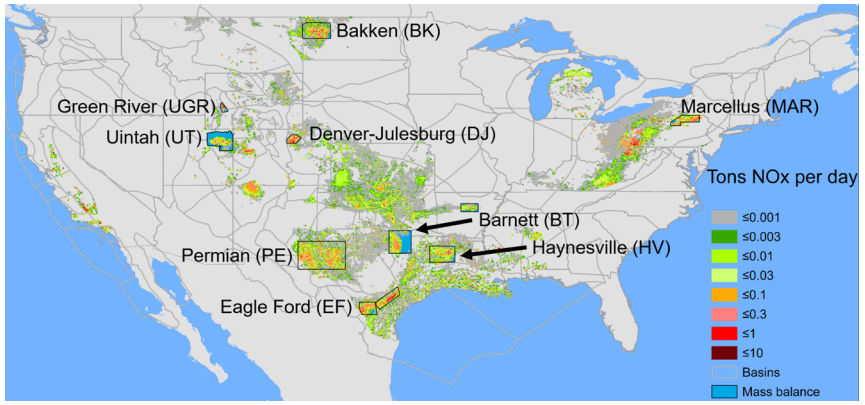

Figure 1. FOG NO_x emissions inventory for 2015. Boxes represent areas where aircraft-derived emissions of CH_4 and NO_y have been estimated. Basin names are labeled along with their abbreviations used later in the study, and gray outlines denote basins using geological information.[58] NO_x emissions are colored on a logarithmic scale. The Permian does not have an associated aircraft-derived emission mass balance, but the box used for Figure 3 is shown for reference.

between these compounds (see Figure 2). Exploring the NO_x/CH_4 emission ratio is also useful as TROPOMI is able to retrieve both NO_2 and CH_4 from space. The NO_x/CH_4 emission ratio can be verified with satellite NO_2/CH_4 in a chemical transport model, where photochemical transformations of NO_x emissions are explicitly accounted.

Following Gorchov Negron et al.,[25] the emission ratio of NO_x to CH_4 is derived from looking at enhancements of the sum of reactive nitrogen (NO_y) and CH_4 over the regional background in individual basins. Nearly all reactive nitrogen emissions from combustion are as NO_x and undergo photochemical processing in the atmosphere to form other nitrogen-containing oxidation products. Thus, we treat ambient NO_y as a conserved measure of NO_x emissions. Large point sources are filtered out by removing spikes three standard deviations above the mean in sulfur dioxide, CO_2, or NO_x. To infer methane emissions in FOG, we use the measured NO_y/CH_4 enhancement ratio. The NOAA P3 aircraft measured many of the US basins with significant production and we extract their respective basin-level NO_y/CH_4 enhancement ratios (ranging from 0.005 to 0.018 mol NO_y/mol CH_4), which account for ∼80% of the grid cells in FOG. In basins without aircraft measurements, ∼20% of the grid cells in FOG, the national average of 0.009 ± 0.002 mol NO_y/mol CH_4 is used.[25] We also check the aircraft ratio of NO_2/CH_4 with TROPOMI satellite correlations reported by de Gouw et al.,[32] who described enhancements of both species observed over the Permian, TX basin. In Figure 2a, we find that the slope of NO_2/CH_4 from the NOAA P3 aircraft in 2015 is within ∼10% of the slope from TROPOMI in 2018. The consistency in the slopes is promising, suggesting that satellite NO_2/CH_4 can potentially constrain fugitive CH_4 emissions, if NO_x emissions can be estimated reliably utilizing the bottom-up fuel-based inventory and NO_x lifetime quantified. A caveat is that it is possible that NO_x/CH_4 emissions could trend overtime, although a long record of co-located NO_x and CH_4 measurements specific to oil and gas regions is limited at this time. While both NO_x and NMVOC[43] emissions are enhanced during drilling, which exhibits high variability due to economic factors,[28] it is possible that relative emissions of NO_x/NMVOC and NO_x/CH_4 could shift during periods of low drilling with sustained production.

The integrated whole air sampler (iWAS) aboard the NOAA P3 aircraft measured NMVOCs, which mainly comprise straight-chained and branched alkanes, cycloalkanes, and aromatics over oil and gas fields.[44] Collection of the canisters occurs over 5 s intervals. We average 1 s CH_4 data over the 5 s time intervals over which the iWAS was collecting NMVOC data. First, we estimate enhancement ratios of individual NMVOCs relative to CH_4 for each basin measured in Figure 1. If an individual NMVOC has a poor correlation with CH_4 (R^2 < 0.3), it was excluded from the analysis. We also omit NMVOCs expected from biogenic sources such as isoprene and monoterpenes. Second, we analyze each individual NMVOC/CH_4 enhancement ratio as a function of the fraction of oil produced, f_{oil} (Table S1). The oil fraction was calculated using well-level oil and gas production statistics from DrillingInfo.[1] In Figure S12, we provide a sample plot of how we calculate $(C_2H_6)/CH_4$ enhancements for an individual basin and then $(C_2H_6)/CH_4$ as a function of oil fraction across all basins. Lastly, benzene and toluene are scaled relative to CH_4 without accounting for oil fraction since these two species were well correlated with CH_4 but did not exhibit a dependence with oil fraction (Table S2).

In Figure 2b, we plot the measured Σ(NMVOC)/CH_4 enhancement ratios versus oil fraction as it is clear that Σ(NMVOC) emissions increase relative to CH_4 as oil fraction increases (R^2 = 0.76). We also plot ethane $(C_2H_6)/CH_4$ in Figure 2b as it is the most abundant NMVOC emitted and exhibits a similar relationship. In regions that predominantly produce oil, referred to as wet basins, the oil is put through a flash tank to separate the liquid- and gas-phase NMVOCs. The gases expelled from the tank are either vented, flared, or collected. Both venting and incomplete combustion from flaring result in the release of NMVOCs directly to the atmosphere.[45] Lastly, to estimate NMVOC emissions for basins without flight data, we use

$$E_{NMVOC} = (1 / X_{NO_y,CH_4}) \cdot (MW_{CH_4}/MW_{NO_y}) \cdot E_{NO_x} \cdot Y_{NMVOC,CH_4} \cdot f_{oil} \quad (1)$$

where E_{NMVOC} is the NMVOC emission for a given basin (g/d), $X_{NOy,CH4}$ is the aircraft-measured molar ratio of NO_y/CH_4 (0.009 ± 0.002 mol NO_y/mol CH_4), MW_{CH4} = 16 g CH_4/mol and MW_{NOy} = 46 g/mol (in NO_2 equivalence), E_{NOx} is the sum of FOG NO_x emissions for a given basin (g/d), f_{oil} is the fraction of oil produced (J/J), and $Y_{NMVOC,CH4}$ is the measured

https://doi.org/10.1021/acs.est.0c07352
Environ. Sci. Technol. 2021, 55, 9129−9139

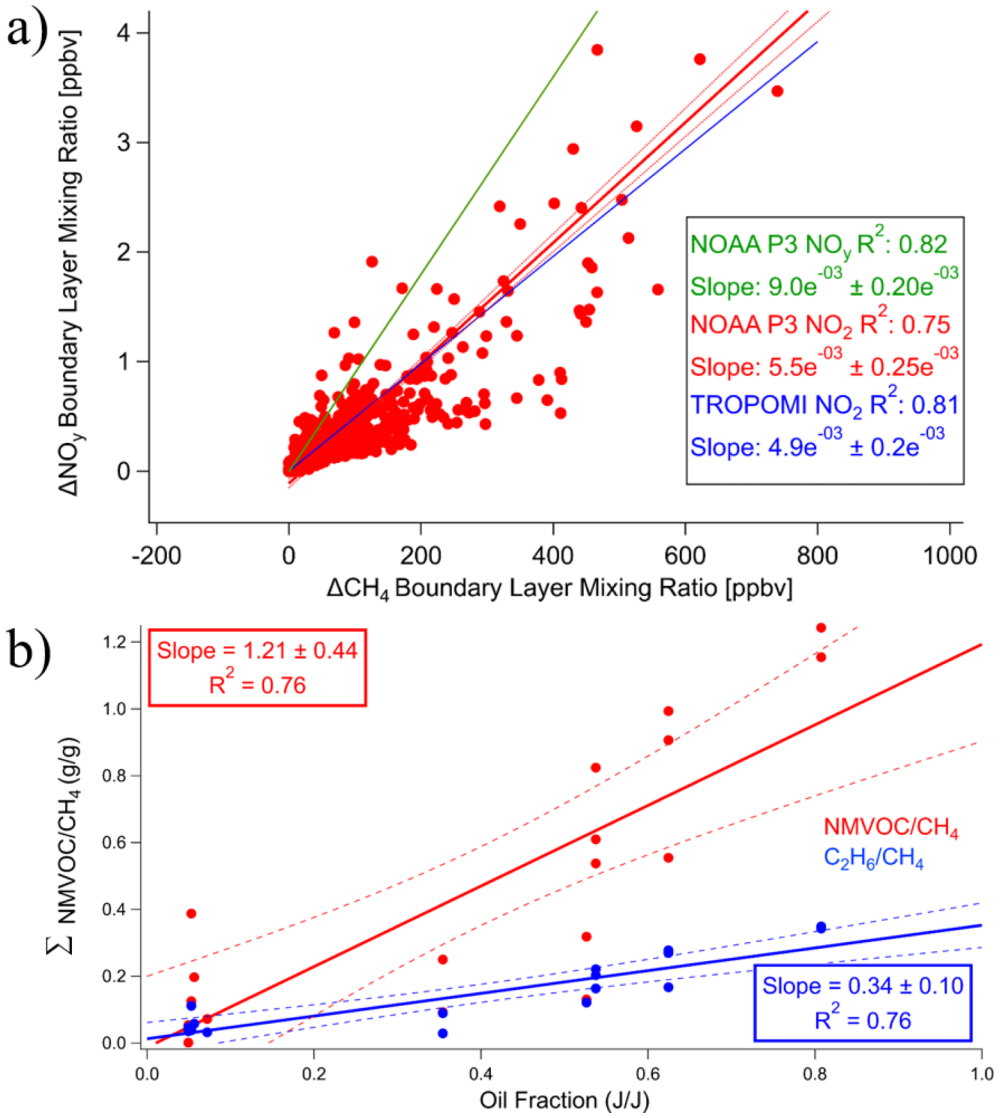

Figure 2. (a) NO_y vs CH_4 and NO_2 vs CH_4 enhancements in the Permian, TX basin from SONGNEX 2015 flights and TROPOMI. The green line represents NO_y/CH_4 as reported in Gorchov Negron et al.[25] The red line represents NO_2/CH_4 estimated in this study. The blue line represents TROPOMI NO_2/CH_4 as reported in de Gouw et al.[32] (b) Correlation between the ratio of ΣNMVOCs to CH_4 vs the oil fraction, f_{oil}, of each basin's production. The markers represent individual basin measurements.

aircraft enhancement ratio of NMVOC/CH_4 as a function of f_{oil} (slope in Figure 2b = 1.26 g NMVOC/g CH_4 per J/J).

We estimate the uncertainty in FOG NO_x emissions using a Monte Carlo analysis following Gorchov Negron et al.,[25] where uncertainty in fuel use and NO_x emission factors are described in detail in Section S3 of Gorchov Negron et al.[25] Here, we report the uncertainty in fuel use and NO_x emission factors by engine type and for each basin in Figures S2−S11. We run 1000 simulations to derive the uncertainty in the basin-level NO_x emission estimate. The largest sources of uncertainty come from wellhead compressors and drill rigs. Additional uncertainties for CH_4 (Figure 2a) and NMVOC (Figure 2b) emissions account for the uncertainty bands in the slopes of the tracer/tracer ratios displayed.

Top-Down Emissions of CH_4 and NO_x. Top-down aircraft-derived emission estimates were quantified for both CH_4 and NO_x for the SENEX 2013 and SONGNEX 2015 field campaigns. The CH_4 concentrations are measured using a Picarro 1301-m CO_2/CH_4 instrument,[46] while NO_y is measured using ozone-induced chemiluminescence.[47]

We perform top-down mass balance emission estimates by determining the difference of concentrations between the area upwind and downwind of oil and gas production regions. A key assumption for the mass balance approach to work is steady winds. The planetary boundary layer height is also a key variable and determined from the vertical profile of potential temperature, ambient temperature, water, CH_4, and C_2H_6. For more information, including boundary layer determination, see Peischl et al.[41,42] A mass balance is performed on measurements of total reactive nitrogen (NO_y), which accounts for all emission sources of NO_x, including mobile sources, power plants, industrial facilities, agriculture, and so forth, in addition to oil and gas production. NO_y mass balances for SENEX flights are based on Gorchov Negron et al.,[25] and here, we expand this analysis to SONGNEX flights as well. Additionally, a mass balance is performed for CH_4.[41,42] The main anthropogenic sources of CH_4 are agriculture, waste, and

https://doi.org/10.1021/acs.est.0c07352
Environ. Sci. Technol. 2021, 55, 9129−9139

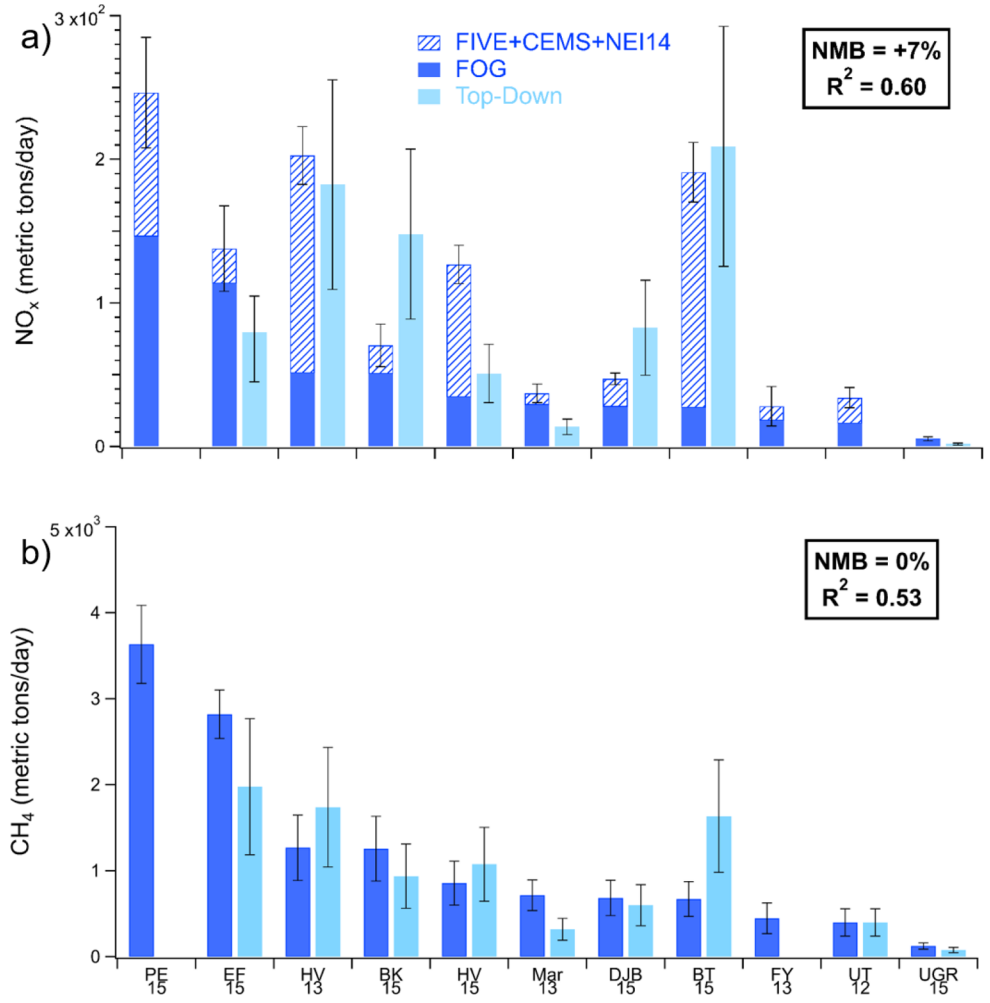

Figure 3. FOG basin-level emission estimates compared with aircraft-derived emissions of NO_x and CH_4 from SENEX 2013[40] and SONGNEX 2015[41,42] flights, as well as the top-down emissions from the UBWOS 2012[12] field campaign in the Uinta Basin. (a) Aircraft NO_x emissions derived utilizing a direct NO_y mass balance (light blue bars), which encompasses all emission sources within the flight domain. Here, the bottom-up emissions (dark blue bars) of FOG are added with emissions from mobile sources (FIVE)[48] and point/area sources (NEI 2014).[49] (b) Oil and natural gas CH_4 emissions inferred from the FOG NO_x inventory compared with the aircraft-derived CH_4 mass balance. The NMB and coefficient of determination (R^2) are shown. Abbreviations: PE = Permian, EF = Eagle Ford, HV = Haynesville, BK = Bakken, MAR = Marcellus, DJB = Denver-Julesburg, BT = Barnett, FY = Fayetteville, UT = Uintah, and UGR = Upper Green River.

industrial processes. However, the P3 aircraft targeted oil and gas regions minimizing the influence of agriculture and waste emissions. In addition, C_2H_6 mass balances allowed for the screening of nonanthropogenic emissions. A top-down estimate of CH_4 is also used from the UBWOS 2012 field campaign.[17] Uncertainty in CH_4 and NMVOC is estimated by using the uncertainty in the NO_y/CH_4 and the NMVOC/CH_4 ratio in every basin. In basins without measurements, we use the national average. Again, the national average is used sparingly due to 80% of the FOG inventory being constrained by flights.

RESULTS AND DISCUSSION

Evaluating FOG NO_x with Aircraft Data. To evaluate the FOG inventory, we compare with aircraft-derived NO_y emission fluxes (that encompass all sources). We use mobile source emissions from the fuel-based inventory of vehicle emissions (FIVEs) described by McDonald et al.[48] Power plant emissions are from the continuous emission monitoring system (CEMS). All other point and area source emissions are from the National Emissions Inventory 2014 (NEI14).[49] In Figure 3a, the aircraft-derived NO_y emissions are compared with total NO_x emissions in the bottom-up inventories (Σ = FOG + FIVE + CEMS + NEI14). To compare the inventories with the aircraft mass balance, we sum only emissions within the area sampled from the aircraft (Figures S2−S11). The coefficient of determination (R^2 = 0.60) and normalized mean bias (NMB) of +7% indicate an overall good performance by the sum of the inventories and not of oil and gas sources alone. In most of the basins shown in Figure 3a (7 out of 10), the oil and gas sector comprises at least half of the NO_x emission budget, and the exception is for those located near cities [e.g., Haynesville (HV), Denver-Julesburg (DJB), and Barnett (BT)]. For urban adjacent basins, the differences in top-down and bottom-up NO_x could be driven by uncertainties in urban emission inventories in these regions, especially for mobile source engines.[48] Regions where NO_x is dominated by oil and gas sources, such as the Eagle Ford (TX), Permian (TX), and Bakken (ND), may explain why prior satellite trend analyses have shown increasing NO_2 columns over time due to the increased oil and gas production.[27−29] Near cities, this trend is likely obscured by the general downward trend of

https://doi.org/10.1021/acs.est.0c07352
Environ. Sci. Technol. 2021, 55, 9129−9139

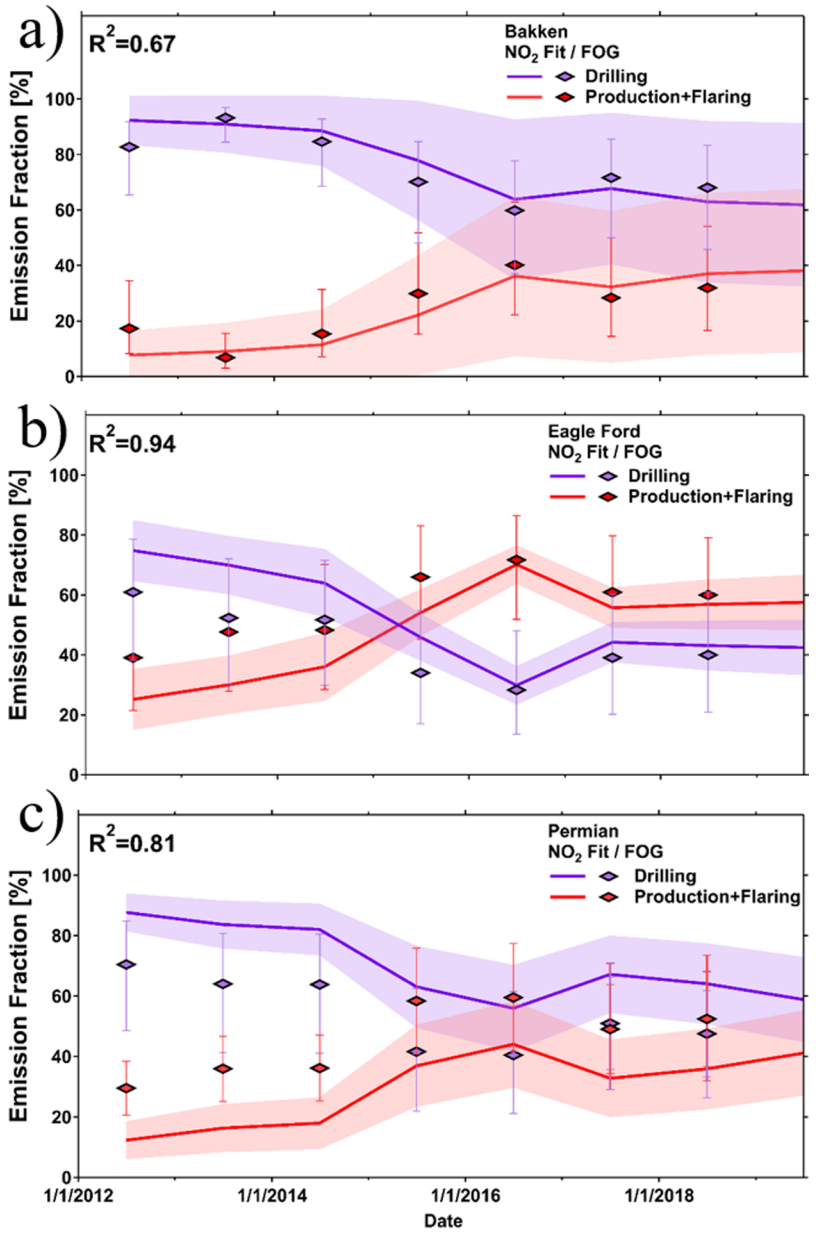

Figure 4. Trend in OMI NO_2 column attributed to drilling (purple line) vs production-phase emissions (red line) shown in Dix et al.[28] for the (a) Bakken, ND, (b) Eagle Ford, TX, and (c) Permian, TX basins. Uncertainty bands reflect the standard deviation. Markers represent the fraction of NO_x emissions from drilling (purple) vs production (red) from the FOG inventory. Error bars represent the maximum and minimum of the drilling and production sector emissions in the bottom-up inventory.

urban NO_x emissions.[12] A caveat is that a mass balance could not be performed in the Permian due to variable winds and underdeveloped boundary layers during the flights. We include the Permian basin since we perform a trend analysis with OMI data in the next section and to illustrate that NO_x emissions in this region are dominated by oil and gas.

While oil and gas production fields are often located near other regional sources of NO_x, CH_4 emissions are much less influenced by non-oil and gas sectors within basins and a more direct measure of oil and gas emissions. Figure 3b shows the emissions of oil and gas CH_4 inferred from the FOG NO_x inventory (=FOG NO_x × aircraft enhancement of CH_4/NO_y) compared with the direct aircraft mass balance of oil and gas emissions of CH_4 from Peischl et al.[40,42] and for the Uinta (UT) Basin.[12,50] In these regions, the CH_4 emissions are dominated by the oil and gas sector, and the inferred CH_4 emissions generally agree with the mass balance estimates (NMB = 0%, R^2 = 0.53). The largest underestimates by FOG occur in the regions without urban influence, while the biggest overestimate occurs in Barnett, which is adjacent to Dallas, TX. In summary, the FOG inventory inferred that CH_4 emissions agree well with aircraft-derived emissions of CH_4 during the field campaign period. Next, we assess how well FOG captures continuous trends in oil and gas NO_x emissions over a longer time period, which is an indicator for the growth of oil and gas production activity over time.

OMI NO_2 Trend Analysis. Expanding on the work of Dix et al.,[28] three regions with increasing NO_2 enhancements observable from space were estimated with FOG between the years of 2012 and 2018. Briefly, Dix et al.[28] correlated trends in drilling activity and oil production with tropospheric NO_2 columns from OMI, which allows for attributing changes in the

https://doi.org/10.1021/acs.est.0c07352
Environ. Sci. Technol. 2021, 55, 9129−9139

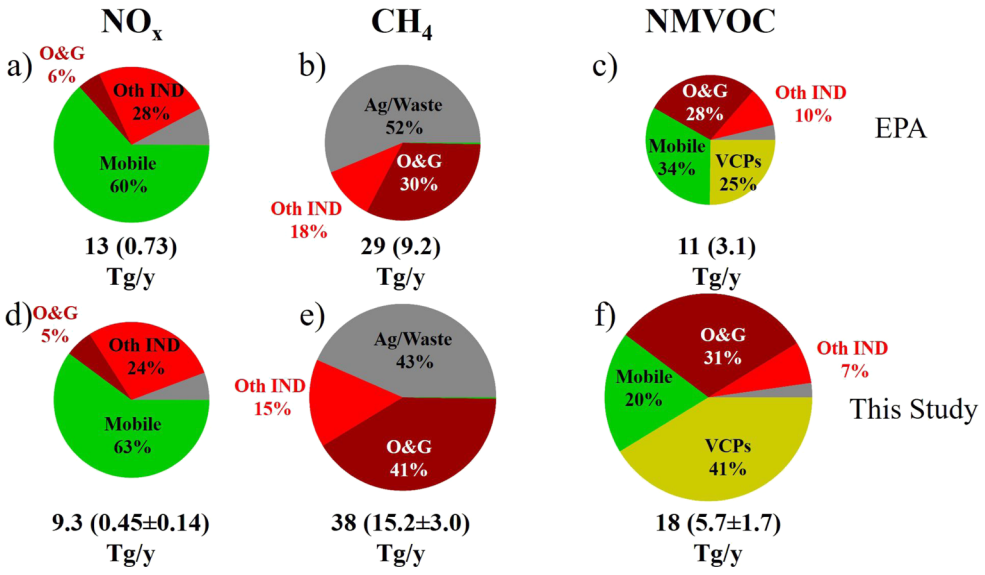

Figure 5. Total 2015 CONUS anthropogenic emissions of NO_x, CH_4, and NMVOCs by source. The top row (a–c) shows emissions reported by the EPA NEI 2014 and GHGI 2015 inventories. The bottom row (d–f) includes the revised oil and gas (O&G) emissions from this study and literature estimates for mobile sources and VCPs.[3,4,48,49,51,59] Other industrial (IND) emissions are from the NEI 2014. Parentheses denote oil and gas emissions in Tg/y.

satellite-observed NO_2 column due to drilling versus production. As shown in Figure 3a, the oil and gas sector dominates NO_x emissions in the Bakken (~72% of total), Eagle Ford (~82% of total), and Permian (~59% of total) basins. This makes these basins prime candidates for analyzing long-term trends of NO_x from oil and gas production. We extract the drilling versus production emissions for these years from the FOG inventory using the same OMI pixel footprint and regression results used in Dix et al.,[28] and results are displayed in Figure 4.

As shown in Figure 4, every point is within the uncertainty of the bottom-up inventory and top-down satellite regression analysis, with the R^2 for the Bakken, Eagle Ford, and Permian being 0.67, 0.94, and 0.81, respectively. The agreement on apportioning NO_x between drilling and production increases the confidence of the FOG inventory in capturing underlying trends in oil and gas emissions over time. Changes in drilling are driven by the price of oil and natural gas. In all three plots, a decrease in drilling is observed due to a drop in the global price of oil in 2014. Different basins have different drilling versus production percentages of NO_x emissions, which is due to a variety of factors, including the ease of extracting oil and natural gas, age of the basin, emission controls, and the amount of natural gas flaring.

Overall, we are able to capture trends in oil and gas NO_x when compared with OMI satellite trends. Future work will explore trends in oil and gas CH_4 and NMVOC emissions. We note that the TROPOMI satellite has simultaneous retrievals of NO_2, formaldehyde, and CH_4, which will allow further exploration of co-emitted NO_x, NMVOC, and CH_4 emissions from oil and gas production since late 2017.[31] The higher spatial resolution of TROPOMI (3.5 km × 7.2 km) versus prior satellites such as OMI (13 km × 24 km) will also allow for a greater capability in distinguishing oil and gas sources separate from other regional sources of emissions. Understanding the trends in drilling and production gives insights into the emissions from oil and gas, as well as tracking efforts to mitigate fugitive leaks of CH_4 and NMVOCs.

CONUS Emissions of NO_x, CH_4, and NMVOCs. We display total estimates of anthropogenic NO_x, CH_4, and NMVOCs in Figure 5 broken down by sectors. The first row shows the EPA NEI 2014[49] emissions across CONUS for NO_x and NMVOCs, along with the EPA GHGI 2015 CH_4 emissions.[51] Only anthropogenic emission sources are shown. The second row revises anthropogenic emissions with the FOG inventory and our estimates of mobile sources based on the FIVE inventory for NO_x and NMVOC emissions.[48,52] Here, we also include recent revisions to NMVOC emissions from volatile chemical products (=coatings, inks, adhesives, personal care products, cleaning agents, etc.), which is likely underestimated by the NEI by a factor of ~3.[52] More information on where the data from other sources originated is found in Tables S3–S5.

The emissions of NO_x from oil and gas production make up only a small fraction of the total US anthropogenic budget (~5%) in Figure 5a,d. While oil and gas NO_x emissions are relatively small at a national scale, basins located near populated areas can contribute to local ozone production.[16,17,53,54] The total revised NO_x emissions are ~30% lower than the NEI 2014 (Figure 5a–d) due to reduced mobile source NO_x emissions in the FIVE inventory by ~25%[48] and ~40% lower oil and gas NO_x emissions in the FOG inventory. This is consistent with the previous comparisons of the FOG inventory with the NEI 2014 by Gorchov Negron et al.[25] and Ahmadov et al.,[12] which found that oil and gas emissions tend to be overestimated by the NEI 2014 in certain basins.

For CH_4, Alvarez et al. also created a bottom-up inventory scaled across the US using facility-level emission factors.[3] The production and drilling emissions from our FOG inventory are 13.1 ± 2.9 Tg/yr of CH_4. The other life cycle emissions of oil and gas use related to processing, transmission, storage, and local distribution were taken from Alvarez et al.[3] and adjusted to avoid double counting of emission sources. Based on the US Greenhouse Gas Reporting Program (GHGRP),[55] we estimate that 5% of local distribution, 35% of refineries, 17% of

https://doi.org/10.1021/acs.est.0c07352
Environ. Sci. Technol. 2021, 55, 9129–9139

transmission and storage, and 78% of processing plants are co-located with the FOG inventory emissions (Figures S13−S16), which we exclude from the summation to obtain the total oil and gas life cycle emission estimate of 15.2 ± 3.0 Tg/yr of CH_4. Alvarez's total CH_4 estimate of 13 (+2.1/−1.7) Tg/yr over the life cycle is within the uncertainty of our estimate. Both inventories suggest that the GHGI significantly underestimates CH_4 emissions from oil and gas production. Inclusion of the FOG inventory increases the total anthropogenic CH_4 emissions over the CONUS by +30%, and the oil and gas contribution increases from 30% to 41% (Figure 5b−e).

Recent studies have quantified the methane emissions of the Permian, TX basin by using an inverse analysis of TROPOMI retrievals. Zhang et al.[56] found emissions from the Permian of 2.7 ± 0.5 Tg CH_4/yr from May 2018 to March 2019. Another study by Schneising et al.[57] over the same period reports an estimate of 2.8 Tg CH_4/yr. Our 2018 inventory over the same domain is 3.4 ± 1.0 Tg CH_4/yr. These results all agree within uncertainty bounds using independent methods. Our study provides another constraint on CH_4 emissions from the Permian, TX, which is the largest onshore oil- and gas-producing region in the lower 48 states.

Due to the underestimate of CH_4 arising from fugitive leaks, it follows that the NEI likely also significantly underestimates NMVOCs from oil and natural gas drilling and production by a factor of ∼2. The distribution of NMVOC emissions does not change significantly (Figure 5c−f), mainly due to the ∼3 times increase in volatile chemical product (VCP) emissions reported by McDonald et al.[48] versus the NEI. However, the total anthropogenic NMVOC emissions increase by ∼7 Tg per year, including a ∼3 Tg increase due to higher oil and gas emissions estimated in this study. As a result, oil and gas emissions remain a significant anthropogenic source of NMVOCs to the atmosphere over the US.

■ ASSOCIATED CONTENT

Supporting Information

The Supporting Information is available free of charge at https://pubs.acs.org/doi/10.1021/acs.est.0c07352.

Equations and methodology used in fuel-based oil and gas inventory; flaring emissions; iWAS species and correlations with oil fraction; iWAS benzene and toluene correlations; data and sources for NO_x, CH_4, and NMVOC; monthly US production of oil and gas; FOG results for Bakken, ND, Barnett, TX, Denver-Julesburg, CO, Eagle Ford, TX, Fayetteville, AR, Haynesville, TX 2015, Haynesville, TX 2013, Marcellus, PA, Upper Green River, WY, and Permian, TX and NM; Permian flight ethane correlation calculation; and GHGRP emissions from refineries, local distribution, processing plants, and transmission and storage (PDF)

■ AUTHOR INFORMATION

Corresponding Author

Brian C. McDonald − *NOAA Chemical Sciences Laboratory, Boulder, Colorado 80305, United States;* orcid.org/0000-0001-8600-5096; Phone: (303) 497-5094; Email: brian.mcdonald@noaa.gov

Authors

Colby B. Francoeur − *Cooperative Institute for Research in Environmental Sciences, University of Colorado Boulder, Boulder, Colorado 80309, United States; NOAA Chemical Sciences Laboratory, Boulder, Colorado 80305, United States;* orcid.org/0000-0003-4491-7462

Jessica B. Gilman − *NOAA Chemical Sciences Laboratory, Boulder, Colorado 80305, United States*

Kyle J. Zarzana − *Cooperative Institute for Research in Environmental Sciences, University of Colorado Boulder, Boulder, Colorado 80309, United States; NOAA Chemical Sciences Laboratory, Boulder, Colorado 80305, United States;* Present Address: Department of Chemistry, University of Colorado Boulder, Boulder, CO 80309, USA.; orcid.org/0000-0003-1581-6419

Barbara Dix − *Cooperative Institute for Research in Environmental Sciences, University of Colorado Boulder, Boulder, Colorado 80309, United States*

Steven S. Brown − *NOAA Chemical Sciences Laboratory, Boulder, Colorado 80305, United States;* orcid.org/0000-0001-7477-9078

Joost A. de Gouw − *Cooperative Institute for Research in Environmental Sciences and Department of Chemistry, University of Colorado Boulder, Boulder, Colorado 80309, United States;* orcid.org/0000-0002-0385-1826

Gregory J. Frost − *NOAA Chemical Sciences Laboratory, Boulder, Colorado 80305, United States*

Meng Li − *Cooperative Institute for Research in Environmental Sciences, University of Colorado Boulder, Boulder, Colorado 80309, United States; NOAA Chemical Sciences Laboratory, Boulder, Colorado 80305, United States*

Stuart A. McKeen − *Cooperative Institute for Research in Environmental Sciences, University of Colorado Boulder, Boulder, Colorado 80309, United States; NOAA Chemical Sciences Laboratory, Boulder, Colorado 80305, United States*

Jeff Peischl − *Cooperative Institute for Research in Environmental Sciences, University of Colorado Boulder, Boulder, Colorado 80309, United States; NOAA Chemical Sciences Laboratory, Boulder, Colorado 80305, United States*

Ilana B. Pollack − *Department of Atmospheric Sciences, Colorado State University, Fort Collins, Colorado 80523, United States*

Thomas B. Ryerson − *NOAA Chemical Sciences Laboratory, Boulder, Colorado 80305, United States;* Present Address: Scientific Aviation, Boulder, CO 80301, USA.

Chelsea Thompson − *Cooperative Institute for Research in Environmental Sciences, University of Colorado Boulder, Boulder, Colorado 80309, United States; NOAA Chemical Sciences Laboratory, Boulder, Colorado 80305, United States*

Carsten Warneke − *Cooperative Institute for Research in Environmental Sciences, University of Colorado Boulder, Boulder, Colorado 80309, United States; NOAA Chemical Sciences Laboratory, Boulder, Colorado 80305, United States;* orcid.org/0000-0003-3811-8496

Michael Trainer − *NOAA Chemical Sciences Laboratory, Boulder, Colorado 80305, United States*

Complete contact information is available at: https://pubs.acs.org/10.1021/acs.est.0c07352

Notes

The authors declare no competing financial interest.

https://doi.org/10.1021/acs.est.0c07352
Environ. Sci. Technol. 2021, 55, 9129−9139

■ ACKNOWLEDGMENTS

This work was supported by NASA ROSES ACMAP (80NSSC19K0979) and NOAA (NA17OAR4320101). Ambient measurements from the SENEX 2013 field study are publicly available at http://www.esrl.noaa.gov/csd/projects/senex/ and from the SONGNEX 2015 field study available at https://www.esrl.noaa.gov/csd/projects/songnex/. The 2015 contiguous FOG inventory for NO_x, CH_4, and NMVOC is provided on the SONGNEX data archive and located at https://csl.noaa.gov/groups/csl7/measurements/2015songnex/emissions/. Drilling and production activity data were provided by Enverus DrillingInfo.

■ REFERENCES

(1) Enverus DrillingInfo. *2020 Future Bid Rounds*, 2020.
(2) Myhre, G.; Shindell, D.; Breon, F. M.; Collins, W.; Fuglestvedt, J.; Huang, J. P.; Koch, D.; Lamarque, J. F.; Lee, D.; Mendoza, B.; Nakajima, T.; Robock, A.; Stephens, G.; Takemura, T.; Zhang, H.; Aamaas, B.; Boucher, O.; Dalsoren, S. B.; Daniel, J. S.; Forster, P.; Granier, C.; Haigh, J.; Hodnebrog, O.; Kaplan, J. O.; Marston, G.; Nielsen, C. J.; O'Neill, B. C.; Peters, G. P.; Pongratz, J.; Prather, M.; Ramaswamy, V.; Roth, R.; Rotstayn, L.; Smith, S. J.; Stevenson, D.; Vernier, J. P.; Wild, O.; Young, P. Anthropogenic and Natural Radiative Forcing. *Climate Change 2013: The Physical Science Basis*; Intergovernmental Panel on Climate Change, 2014; pp 659−740.
(3) Alvarez, R. A.; Zavala-Araiza, D.; Lyon, D. R.; Allen, D. T.; Barkley, Z. R.; Brandt, A. R.; Davis, K. J.; Herndon, S. C.; Jacob, D. J.; Karion, A.; Kort, E. A.; Lamb, B. K.; Lauvaux, T.; Maasakkers, J. D.; Marchese, A. J.; Omara, M.; Pacala, S. W.; Peischl, J.; Robinson, A. L.; Shepson, P. B.; Sweeney, C.; Townsend-Small, A.; Wofsy, S. C.; Hamburg, S. P. Assessment of methane emissions from the US oil and gas supply chain. *Science* **2018**, *361*, 186−188.
(4) Plant, G.; Kort, E. A.; Floerchinger, C.; Gvakharia, A.; Vimont, I.; Sweeney, C. Large Fugitive Methane Emissions From Urban Centers Along the US East Coast. *Geophys. Res. Lett.* **2019**, *46*, 8500−8507.
(5) Lan, X.; Tans, P.; Sweeney, C.; Andrews, A.; Dlugokencky, E.; Schwietzke, S.; Kofler, J.; McKain, K.; Thoning, K.; Crotwell, M.; Montzka, S.; Miller, B. R.; Biraud, S. C. Long-Term Measurements Show Little Evidence for Large Increases in Total US Methane Emissions Over the Past Decade. *Geophys. Res. Lett.* **2019**, *46*, 4991−4999.
(6) Schwietzke, S.; Sherwood, O. A.; Bruhwiler, L. M. P.; Miller, J. B.; Etiope, G.; Dlugokencky, E. J.; Michel, S. E.; Arling, V. A.; Vaughn, B. H.; White, J. W. C.; Tans, P. P. Upward revision of global fossil fuel methane emissions based on isotope database. *Nature* **2016**, *538*, 88−91.
(7) Simpson, I. J.; Sulbaek Andersen, M. P.; Meinardi, S.; Bruhwiler, L.; Blake, N. J.; Helmig, D.; Rowland, F. S.; Blake, D. R. Long-term decline of global atmospheric ethane concentrations and implications for methane. *Nature* **2012**, *488*, 490−494.
(8) Turner, A. J.; Jacob, D. J.; Benmergui, J.; Wofsy, S. C.; Maasakkers, J. D.; Butz, A.; Hasekamp, O.; Biraud, S. C. A large increase in US methane emissions over the past decade inferred from satellite data and surface observations. *Geophys. Res. Lett.* **2016**, *43*, 2218−2224.
(9) Bell, M. L.; McDermott, A.; Zeger, S. L.; Samet, J. M.; Dominici, F. Ozone and short-term mortality in 95 US urban communities, 1987-2000. *JAMA, J. Am. Med. Assoc.* **2004**, *292*, 2372−2378.
(10) Jerrett, M.; Burnett, R. T.; Pope, C. A.; Ito, K.; Thurston, G.; Krewski, D.; Shi, Y.; Calle, E.; Thun, M. Long-Term Ozone Exposure and Mortality. *N. Engl. J. Med.* **2009**, *360*, 1085−1095.
(11) Cheadle, L. C.; Oltmans, S. J.; Petron, G.; Schnell, R. C.; Mattson, E. J.; Herndon, S. C.; Thompson, A. M.; Blake, D. R.; McClure-Begley, A. Surface ozone in the Colorado northern Front Range and the influence of oil and gas development during FRAPPE/DISCOVER-AQ in summer 2014. *Elementa-Sci. Anthrop.* **2017**, *5*, 61.
(12) Ahmadov, R.; McKeen, S.; Trainer, M.; Banta, R.; Brewer, A.; Brown, S.; Edwards, P. M.; de Gouw, J. A.; Frost, G. J.; Gilman, J.; Helmig, D.; Johnson, B.; Karion, A.; Koss, A.; Langford, A.; Lerner, B.; Olson, J.; Oltmans, S.; Peischl, J.; Pétron, G.; Pichugina, Y.; Roberts, J. M.; Ryerson, T.; Schnell, R.; Senff, C.; Sweeney, C.; Thompson, C.; Veres, P. R.; Warneke, C.; Wild, R.; Williams, E. J.; Yuan, B.; Zamora, R. Understanding high wintertime ozone pollution events in an oil- and natural gas-producing region of the western US. *Atmos. Chem. Phys.* **2015**, *15*, 411−429.
(13) Edwards, P. M.; Brown, S. S.; Roberts, J. M.; Ahmadov, R.; Banta, R. M.; deGouw, J. A.; Dubé, W. P.; Field, R. A.; Flynn, J. H.; Gilman, J. B.; Graus, M.; Helmig, D.; Koss, A.; Langford, A. O.; Lefer, B. L.; Lerner, B. M.; Li, R.; Li, S.-M.; McKeen, S. A.; Murphy, S. M.; Parrish, D. D.; Senff, C. J.; Soltis, J.; Stutz, J.; Sweeney, C.; Thompson, C. R.; Trainer, M. K.; Tsai, C.; Veres, P. R.; Washenfelder, R. A.; Warneke, C.; Wild, R. J.; Young, C. J.; Yuan, B.; Zamora, R. High winter ozone pollution from carbonyl photolysis in an oil and gas basin. *Nature* **2014**, *514*, 351.
(14) Schnell, R. C.; Johnson, B. J.; Oltmans, S. J.; Cullis, P.; Sterling, C.; Hall, E.; Jordan, A.; Helmig, D.; Petron, G.; Ahmadov, R.; Wendell, J.; Albee, R.; Boylan, P.; Thompson, C. R.; Evans, J.; Hueber, J.; Curtis, A. J.; Park, J. H. Quantifying wintertime boundary layer ozone production from frequent profile measurements in the Uinta Basin, UT, oil and gas region. *J. Geophys. Res. Atmos.* **2016**, *121*, 11038−11054.
(15) Dalsøren, S. B.; Myhre, G.; Hodnebrog, O.; Myhre, C. L.; Stohl, A.; Pisso, I.; Schwietzke, S.; Hoglund-Isaksson, L.; Helmig, D.; Reimann, S.; Sauvage, S.; Schmidbauer, N.; Read, K. A.; Carpenter, L. J.; Lewis, A. C.; Punjabi, S.; Wallasch, M. Discrepancy between simulated and observed ethane and propane levels explained by underestimated fossil emissions. *Nat. Geosci.* **2018**, *11*, 178.
(16) McDuffie, E. E.; Edwards, P. M.; Gilman, J. B.; Lerner, B. M.; Dubé, W. P.; Trainer, M.; Wolfe, D. E.; Angevine, W. M.; deGouw, J.; Williams, E. J.; Tevlin, A. G.; Murphy, J. G.; Fischer, E. V.; McKeen, S.; Ryerson, T. B.; Peischl, J.; Holloway, J. S.; Aikin, K.; Langford, A. O.; Senff, C. J.; Alvarez, R. J.; Hall, S. R.; Ullmann, K.; Lantz, K. O.; Brown, S. S. Influence of oil and gas emissions on summertime ozone in the Colorado Northern Front Range. *J. Geophys. Res. Atmos.* **2016**, *121*, 8712−8729.
(17) Gilman, J. B.; Lerner, B. M.; Kuster, W. C.; de Gouw, J. A. Source Signature of Volatile Organic Compounds from Oil and Natural Gas Operations in Northeastern Colorado. *Environ. Sci. Technol.* **2013**, *47*, 1297−1305.
(18) Abdi-Oskouei, M.; Pfister, G.; Flocke, F.; Sobhani, N.; Saide, P.; Fried, A.; Richter, D.; Weibring, P.; Walega, J.; Carmichael, G. Impacts of physical parameterization on prediction of ethane concentrations for oil and gas emissions in WRF-Chem. *Atmos. Chem. Phys.* **2018**, *18*, 16863−16883.
(19) Pfister, G.; Wang, C. T.; Barth, M.; Flocke, F.; Vizuete, W.; Walters, S. Chemical Characteristics and Ozone Production in the Northern Colorado Front Range. *J. Geophys. Res. Atmos.* **2019**, *124*, 13397−13419.
(20) Pozzer, A.; Schultz, M. G.; Helmig, D. Impact of U.S. Oil and Natural Gas Emission Increases on Surface Ozone Is Most Pronounced in the Central United States. *Environ. Sci. Technol.* **2020**, *54*, 12423−12433.
(21) Kort, E. A.; Smith, M. L.; Murray, L. T.; Gvakharia, A.; Brandt, A. R.; Peischl, J.; Ryerson, T. B.; Sweeney, C.; Travis, K. Fugitive emissions from the Bakken shale illustrate role of shale production in global ethane shift. *Geophys. Res. Lett.* **2016**, *43*, 4617−4623.
(22) Benedict, K. B.; Prenni, A. J.; El-Sayed, M. M. H.; Hecobian, A.; Zhou, Y.; Gebhart, K. A.; Sive, B. C.; Schichtel, B. A.; Collett, J. L. Volatile organic compounds and ozone at four national parks in the southwestern United States. *Atmos. Environ.* **2020**, *239*, 117783.
(23) Evanoski-Cole, A. R.; Gebhart, K. A.; Sive, B. C.; Zhou, Y.; Capps, S. L.; Day, D. E.; Prenni, A. J.; Schurman, M. I.; Sullivan, A. P.; Li, Y.; Hand, J. L.; Schichtel, B. A.; Collett, J. L. Composition and sources of winter haze in the Bakken oil and gas extraction region. *Atmos. Environ.* **2017**, *156*, 77−87.

https://doi.org/10.1021/acs.est.0c07352
Environ. Sci. Technol. 2021, 55, 9129−9139

(24) Prenni, A. J.; Day, D. E.; Evanoski-Cole, A. R.; Sive, B. C.; Hecobian, A.; Zhou, Y.; Gebhart, K. A.; Hand, J. L.; Sullivan, A. P.; Li, Y.; Schurman, M. I.; Desyaterik, Y.; Malm, W. C.; Collett, J. L., Jr.; Schichtel, B. A. Oil and gas impacts on air quality in federal lands in the Bakken region: an overview of the Bakken Air Quality Study and first results. *Atmos. Chem. Phys.* **2016**, *16*, 1401−1416.
(25) Gorchov Negron, A. M.; McDonald, B. C.; McKeen, S. A.; Peischl, J.; Ahmadov, R.; de Gouw, J. A.; Frost, G. J.; Hastings, M. G.; Pollack, I. B.; Ryerson, T. B.; Thompson, C.; Warneke, C.; Trainer, M. Development of a Fuel-Based Oil and Gas Inventory of Nitrogen Oxides Emissions. *Environ. Sci. Technol.* **2018**, *52*, 10175−10185.
(26) Carlton, A. G.; Little, E.; Moeller, M.; Odoyo, S.; Shepson, P. B. The Data Gap: Can a Lack of Monitors Obscure Loss of Clean Air Act Benefits in Fracking Areas? *Environ. Sci. Technol.* **2014**, *48*, 893−894.
(27) Duncan, B. N.; Lamsal, L. N.; Thompson, A. M.; Yoshida, Y.; Lu, Z.; Streets, D. G.; Hurwitz, M. M.; Pickering, K. E. A space-based, high-resolution view of notable changes in urban NOx pollution around the world (2005-2014). *J. Geophys. Res. Atmos.* **2016**, *121*, 976−996.
(28) Dix, B.; de Bruin, J.; Roosenbrand, E.; Vlemmix, T.; Francoeur, C.; Gorchov-Negron, A.; McDonald, B.; Zhizhin, M.; Elvidge, C.; Veefkind, P.; Levelt, P.; de Gouw, J. Nitrogen Oxide Emissions from U.S. Oil and Gas Production: Recent Trends and Source Attribution. *Geophys. Res. Lett.* **2020**, *47*, No. e2019GL085866.
(29) Majid, A.; Martin, M. V.; Lamsal, L. N.; Duncan, B. N. A decade of changes in nitrogen oxides over regions of oil and natural gas activity in the United States. *Elementa-Sci. Anthrop.* **2017**, *5*, 76.
(30) Streets, D. G.; Canty, T.; Carmichael, G. R.; de Foy, B.; Dickerson, R. R.; Duncan, B. N.; Edwards, D. P.; Haynes, J. A.; Henze, D. K.; Houyoux, M. R.; Jacob, D. J.; Krotkov, N. A.; Lamsal, L. N.; Liu, Y.; Lu, Z.; Martin, R. V.; Pfister, G. G.; Pinder, R. W.; Salawitch, R. J.; Wecht, K. J. Emissions estimation from satellite retrievals: A review of current capability. *Atmos. Environ.* **2013**, *77*, 1011−1042.
(31) Veefkind, J. P.; Aben, I.; McMullan, K.; Förster, H.; de Vries, J.; Otter, G.; Claas, J.; Eskes, H. J.; de Haan, J. F.; van Weele, M.; Hasekamp, O.; Hoogeveen, R.; Landgraf, J.; Snel, R.; Tol, P.; Ingmann, P.; Voors, R.; Kruizinga, B.; Vink, R.; Visser, H.; Levelt, P. F.; Levelt, P. F. TROPOMI on the ESA Sentinel-5 Precursor: A GMES mission for global observations of the atmospheric composition for climate, air quality and ozone layer applications. *Remote Sens. Environ.* **2012**, *120*, 70−83.
(32) de Gouw, J. A.; Veefkind, J. P.; Roosenbrand, E.; Dix, B.; Lin, J. C.; Landgraf, J.; Levelt, P. F. Daily Satellite Observations of Methane from Oil and Gas Production Regions in the United States. *Sci. Rep.* **2020**, *10*, 1379.
(33) Elvidge, C. D.; Zhizhin, M.; Baugh, K.; Hsu, F. C.; Ghosh, T. Methods for Global Survey of Natural Gas Flaring from Visible Infrared Imaging Radiometer Suite Data. *Energies* **2016**, *9*, 14.
(34) Energy Information Administration. *Distillate Fuel Oil and Kerosene Sales by End Use*, 2020.
(35) Energy Information Administration. *Natural Gas Consumption by End Use: Lease Fuel Consumption*, 2020.
(36) U.S. Environmental Protection Agency. *Oil and Gas 101: An Overview of Oil and Gas Upstream Activities and Using EPA's Nonpoint Oil and Gas Emission Estimation Tool for the 2017 NEI*, 2017. https://www.epa.gov/sites/production/files/2017-10/documents/oil_and_gas_101_training_8_15_17.pdf.
(37) Environmental Protection Agency. *EPA Nonpoint Oil and Gas Emission Estimation Tool for the 2014 NEI*, 2015.
(38) Torres, V. M.; Herndon, S.; Wood, E.; Al-Fadhli, F. M.; Allen, D. T. Emissions of Nitrogen Oxides from Flares Operating at Low Flow Conditions. *Ind. Eng. Chem. Res.* **2012**, *51*, 12600−12605.
(39) Zhang, Y.; Gautam, R.; Zavala-Araiza, D.; Jacob, D. J.; Zhang, R.; Zhu, L.; Sheng, J. X.; Scarpelli, T. Satellite-Observed Changes in Mexico's Offshore Gas Flaring Activity Linked to Oil/Gas Regulations. *Geophys. Res. Lett.* **2019**, *46*, 1879−1888.
(40) Peischl, J.; Ryerson, T. B.; Aikin, K. C.; Gouw, J. A.; Gilman, J. B.; Holloway, J. S.; Lerner, B. M.; Nadkarni, R.; Neuman, J. A.; Nowak, J. B.; Trainer, M.; Warneke, C.; Parrish, D. D. Quantifying atmospheric methane emissions from the Haynesville, Fayetteville, and northeastern Marcellus shale gas production regions. *J. Geophys. Res. Atmos.* **2015**, *120*, 2119−2139.
(41) Peischl, J.; Karion, A.; Sweeney, C.; Kort, E. A.; Smith, M. L.; Brandt, A. R.; Yeskoo, T.; Aikin, K. C.; Conley, S. A.; Gvakharia, A.; Trainer, M.; Wolter, S.; Ryerson, T. B. Quantifying atmospheric methane emissions from oil and natural gas production in the Bakken shale region of North Dakota. *J. Geophys. Res. Atmos.* **2016**, *121*, 6101−6111.
(42) Peischl, J.; Eilerman, S. J.; Neuman, J. A.; Aikin, K. C.; de Gouw, J.; Gilman, J. B.; Herndon, S. C.; Nadkarni, R.; Trainer, M.; Warneke, C.; Ryerson, T. B. Quantifying Methane and Ethane Emissions to the Atmosphere From Central and Western US Oil and Natural Gas Production Regions. *J. Geophys. Res. Atmos.* **2018**, *123*, 7725−7740.
(43) Hecobian, A.; Clements, A. L.; Shonkwiler, K. B.; Zhou, Y.; MacDonald, L. P.; Hilliard, N.; Wells, B. L.; Bibeau, B.; Ham, J. M.; Pierce, J. R.; Collett, J. L. Air Toxics and Other Volatile Organic Compound Emissions from Unconventional Oil and Gas Development. *Environ. Sci. Technol. Lett.* **2019**, *6*, 720−726.
(44) Lerner, B. M.; Gilman, J. B.; Aikin, K. C.; Atlas, E. L.; Goldan, P. D.; Graus, M.; Hendershot, R.; Isaacman-VanWertz, G. A.; Koss, A.; Kuster, W. C.; Lueb, R. A.; McLaughlin, R. J.; Peischl, J.; Sueper, D.; Ryerson, T. B.; Tokarek, T. W.; Warneke, C.; Yuan, B.; de Gouw, J. A. An improved, automated whole air sampler and gas chromatography mass spectrometry analysis system for volatile organic compounds in the atmosphere. *Atmos. Meas. Tech.* **2017**, *10*, 291−313.
(45) Department of Energy. *Natural Gas Flaring and Venting: State and Federal Regulatory Overview, Trends, and Impacts*, 2019.
(46) Peischl, J.; Ryerson, T. B.; Holloway, J. S.; Trainer, M.; Andrews, A. E.; Atlas, E. L.; Blake, D. R.; Daube, B. C.; Dlugokencky, E. J.; Fischer, M. L.; Goldstein, A. H.; Guha, A.; Karl, T.; Kofler, J.; Kosciuch, E.; Misztal, P. K.; Perring, A. E.; Pollack, I. B.; Santoni, G. W.; Schwarz, J. P.; Spackman, J. R.; Wofsy, S. C.; Parrish, D. D. Airborne observations of methane emissions from rice cultivation in the Sacramento Valley of California. *J. Geophys. Res. Atmos.* **2012**, *117*, D00V25.
(47) Ryerson, T. B.; Huey, L. G.; Knapp, K.; Neuman, J. A.; Parrish, D. D.; Sueper, D. T.; Fehsenfeld, F. C. Design and initial characterization of an inlet for gas-phase NOy measurements from aircraft. *J. Geophys. Res. Atmos.* **1999**, *104*, 5483−5492.
(48) McDonald, B. C.; McKeen, S. A.; Cui, Y. Y.; Ahmadov, R.; Kim, S.-W.; Frost, G. J.; Pollack, I. B.; Peischl, J.; Ryerson, T. B.; Holloway, J. S.; Graus, M.; Warneke, C.; Gilman, J. B.; de Gouw, J. A.; Kaiser, J.; Keutsch, F. N.; Hanisco, T. F.; Wolfe, G. M.; Trainer, M. Modeling Ozone in the Eastern US using a Fuel-Based Mobile Source Emissions Inventory. *Environ. Sci. Technol.* **2018**, *52*, 7360−7370.
(49) Environmental Protection Agency. *National Emissions Inventory (NEI) 2014*, version 1; Office of Air Quality Planning and Standards, 2017.
(50) Karion, A.; Sweeney, C.; Pétron, G.; Frost, G.; Michael Hardesty, R.; Kofler, J.; Miller, B. R.; Newberger, T.; Wolter, S.; Banta, R.; Brewer, A.; Dlugokencky, E.; Lang, P.; Montzka, S. A.; Schnell, R.; Tans, P.; Trainer, M.; Zamora, R.; Conley, S. Methane emissions estimate from airborne measurements over a western United States natural gas field. *Geophys. Res. Lett.* **2013**, *40*, 4393−4397.
(51) *Environmental Protection Agency: Inventory of U.S. Greenhouse Gas Emissions and Sinks*; U.S. EPA, 2020.
(52) McDonald, B. C.; de Gouw, J. A.; Gilman, J. B.; Jathar, S. H.; Akherati, A.; Cappa, C. D.; Jimenez, J. L.; Lee-Taylor, J.; Hayes, P. L.; McKeen, S. A.; Cui, Y. Y.; Kim, S.-W.; Gentner, D. R.; Isaacman-VanWertz, G.; Goldstein, A. H.; Harley, R. A.; Frost, G. J.; Roberts, J. M.; Ryerson, T. B.; Trainer, M. Volatile chemical products emerging

https://doi.org/10.1021/acs.est.0c07352
Environ. Sci. Technol. 2021, 55, 9129−9139

as largest petrochemical source of urban organic emissions. *Science* **2018**, *359*, 760−764.
(53) Abeleira, A.; Pollack, I. B.; Sive, B.; Zhou, Y.; Fischer, E. V.; Farmer, D. K. Source characterization of volatile organic compounds in the Colorado Northern Front Range Metropolitan Area during spring and summer 2015. *J. Geophys. Res. Atmos.* **2017**, *122*, 3595−3613.
(54) Abeleira, A. J.; Farmer, D. K. Summer ozone in the northern Front Range metropolitan area: weekend-weekday effects, temperature dependences, and the impact of drought. *Atmos. Chem. Phys.* **2017**, *17*, 6517−6529.
(55) Environmental Protection Agency. *Greenhouse Gas Reporting Program*, 2021. https://www.epa.gov/ghgreporting.
(56) Zhang, Y.; Gautam, R.; Pandey, S.; Omara, M.; Maasakkers, J. D.; Sadavarte, P.; Lyon, D.; Nesser, H.; Sulprizio, M. P.; Varon, D. J.; Zhang, R. X.; Houweling, S.; Zavala-Araiza, D.; Alvarez, R. A.; Lorente, A.; Hamburg, S. P.; Aben, I.; Jacob, D. J. Quantifying methane emissions from the largest oil-producing basin in the United States from space. *Sci. Adv.* **2020**, *6*, No. eaaz5120.
(57) Schneising, O.; Buchwitz, M.; Reuter, M.; Vanselow, S.; Bovensmann, H.; Burrows, J. P. Remote sensing of methane leakage from natural gas and petroleum systems revisited. *Atmos. Chem. Phys.* **2020**, *20*, 9169.
(58) Robertson_CGG. *Sedimentary Basins of the World*, 2020.
(59) Jiang, Z.; McDonald, B. C.; Worden, H.; Worden, J. R.; Miyazaki, K.; Qu, Z.; Henze, D. K.; Jones, D. B. A.; Arellano, A. F.; Fischer, E. V.; Zhu, L.; Boersma, K. F. Unexpected slowdown of US pollutant emission reduction in the past decade. *Proc. Natl. Acad. Sci. U.S.A.* **2018**, *115*, 5099−5104.

https://doi.org/10.1021/acs.est.0c07352
Environ. Sci. Technol. 2021, 55, 9129−9139